Bulletin of the Seismological Society of America, 90, 4, pp. 1062–1081, August 2000

Ground-Motion Scaling in the Apennines (Italy)

by Luca Malagnini, Robert B. Herrmann, and Massimo Di Bona

Abstract Regressions over a data set of broadband seismograms are performed to quantify the attenuation of the ground motion in the Apennines (Italy), in the 0.25–5.0 Hz frequency band. The data set used in this article consists of over 6000 horizontal-component seismograms from 446 events, with magnitude ranging from $M_w \simeq 2$ to $M_w = 6.0$. Waveforms were collected during recent field experiments along the Apennines. Data from two MedNet broadband stations, located in central and southern Apennines, were also used.

Seismograms are bandpass-filtered around a set of sampling frequencies, and the logarithms of their peak values are written as

$$\mathrm{AMP}(f, r) = \mathrm{EXC}(f, r_{\mathrm{ref}}) + \mathrm{SITE}(f) + D(r, r_{\mathrm{ref}}, f).$$

$\mathrm{EXC}(f, r_{\mathrm{ref}})$ is the excitation term for the ground motion at the hypocentral distance r_{ref}. $\mathrm{SITE}(f)$ represents the distortion of the seismic spectra induced by the shallow geology at the recording site. $D(r, r_{\mathrm{ref}}, f)$ includes the effects of the geometrical spreading, $g(r)$, and of a frequency-dependent crustal attenuation Q. It is determined as a piecewise linear function, allowing to consider complex behavior of the regional attenuation.

A first estimate of $D(r, r_{\mathrm{ref}}, f)$ is obtained using a coda normalization technique (Aki, 1980; Frankel *et al.,* 1990) and used as a starting model in the inversion of the peak values. Then, by trial and error, the empirical $D(r, r_{\mathrm{ref}}, f)$ is fitted using a trilinear geometrical spreading, with crossover distances at 30 and 80 km, and the crustal parameter

$$Q(f) = 130 \left(\frac{f}{f_{\mathrm{ref}}}\right)^{0.10}; f_{\mathrm{ref}} = 1.0 \text{ Hz}$$

These results suggest a low-Q crust in the entire Apennines in the 0.25–5.0 Hz range, implying that the seismic hazard in the region may be dominated by the local seismicity.

The final section is devoted to highlight the limitations of the formula proposed by Console *et al.* (1988) to estimate duration magnitudes M_d in Italy.

Introduction

The assessment of seismic hazard is probably the most important contribution of seismology to society. The prediction of the earthquake ground motion has always been of primary interest for seismologists and structural engineers. A deterministic approach is done by matching shape and amplitude of every single pulse in the seismograms. This point of view is very important in seismology, since it allows us to obtain important information about the seismic source, and also a quantitative description of the medium through which the energy propagates. Although waveform modeling is widely and successfully used in global, long-period seismology, and even at regional distance, a different approach must be used to describe the high-frequency ground motion at short distances from the source because the complexity of the physical system (i.e., the rupturing fault coupled with a strongly heterogeneous Earth) goes beyond a critical level. In treating high-frequency strong ground motion recordings (accelerograms), we thus require a statistical approach. Instead of trying to reproduce the details of the ground acceleration in the time domain, we use a source model and a regional scaling law to predict its spectral shape and amplitudes at various source-receiver distances. Peak values in the

time domain are predicted by exploiting the stochastic nature of the accelerograms.

In this article we will deal mostly with ground velocity data, but the results of our regressions will be of general interest and will be applicable to the prediction of either the peaks or the spectral amplitudes of ground acceleration, velocity, displacement, or of the corresponding response spectra. For what follows, we will assume that each time series of our data set represents the actual ground motion (velocity), retrieved from the original data by carefully removing the distortion induced by the recording system.

The quantitative estimate of the ground motion is obtained through the use of the so-called predictive relationships (see Kramer, 1996), which allow the computation of specific ground-motion parameter as a function of magnitude, distance from the source, and frequency. They are obtained by multiplying the far-field source spectrum (Brune, 1970, 1971; Boore, 1983; Atkinson and Boore, 1995) at different magnitudes, with the empirical estimate of the regional attenuation of the ground motion. Additional factors will take care of the spectral distortion induced by the shallow geology. Predictive relationships need to be calibrated over the region of interest. In this article we will deal primarily with the calibration of an empirical crustal attenuation function, although we will also provide some discussion on the source spectra evaluation.

A statistical tool called random vibration theory (RVT, see Cartwright and Longuet-Higgins, 1956, for a general formulation in terms of spectral shape and signal duration) allows us to estimate the peak value of a random time history (e.g., acceleration), given its spectrum and its duration in time. If we know the regional scaling law at different frequencies, we can project the acceleration spectrum to the desired hypocentral distance from the source and predict the PHA at the site of interest. It is worth mentioning other seismological application of RVT by Udwadia and Trifunac (1974) and Vanmarcke and Lai (1980). Clough and Penzien (1975) analyze applications of RVT in a structural engineering context.

Alternatively, a simulation method proposed by Boore (1983) can be used. In this method, by averaging over many pseudo-random acceleration waveforms, we can obtain the parameters of the statistical distribution for the PHA as a function of frequency and magnitude. Again, the knowledge of the regional scaling relationships is required to make a prediction for the PHA at the desired distance.

A precise evaluation of the duration of the ground motion at a specific site is extremely important for two reasons: (1) it is an input parameter for RVT; and (2) duration is a critical parameter in triggering liquefaction phenomena, whereas relatively low values of PHA are necessary for liquefaction to occur (0.1 *g*, see Kramer, 1996).

Duration is a function of the fault size (i.e., the duration of the rupture) and of the dispersion that elastic waves experience along source-receiver paths. Scattering also contributes to the increase of duration at increasing distances from the source. Dispersion redistributes in time the frequency content of the radiated spectrum in a way that is deterministically predictable in theory if the structure of the medium is known. On the other hand, scattering redistributes the seismic energy in space and time, behind the wavefronts, during a stochastic process that is treated in a statistical fashion, even with diffusion equations if the scattering is strong enough. We can see here a clear analogy with the kinetic theory of gases, since mean free paths can be defined also for the elastic waves scattered through the Earth, as well as for the gas molecules confined at a certain pressure and temperature (Aki and Chouet, 1975; Wu, 1985; Hoshiba, 1991). The estimate of the duration of the signals as a function of distance from the source can be obtained empirically from the data, provided an unambiguous definition of the duration itself. For the signal that follows the *S* waves, Atkinson and Boore (1995) defined duration so that the observed peak for each time history agrees with the corresponding RVT prediction. Raoof *et al.* (1999) used the integral of the seismic energy, starting from the *S*-wave onset, and defined duration as time window that brackets the 5%–75% fraction of this energy. The choice of duration estimate contains some level of subjective judgment. The definition of duration has very important practical implications, since we need to develop fully automated procedures that include a proper signal windowing in the time domain, when processing very large amounts of data. We also use the 5%–75% time window as a measure of effective signal duration.

Seismological Characteristics of the Apennines

The characteristics of the seismic sources and of the crustal attenuation in the Apennines have been investigated in previous studies. Rovelli *et al.* (1988) analyzed 75 strong-motion accelerograms from the Central and the Southern Apennines ($4 \leq M \leq 7$), all from normal faulting, in the $0.1 \leq f \leq 20$ Hz spectral band. By using a ω^2 model to match the observed acceleration spectra, they investigated the source parameters M_0 (the seismic moment) and f_c (the corner frequency). The parameter κ (Anderson and Hough, 1984) was also quantified, after forcing a linear dependence on frequency for the crustal attenuation parameter $Q(f) = Q_0(f/f_{\text{ref}})$, with $Q_0 = 100$ and $f_{\text{ref}} = 1.0$ Hz. Rovelli *et al.* (1988) also verified the "cube root" corner frequency-seismic moment relationship for the events along the Apennines, and the value of the Brune stress drop

$$\Delta\sigma = 190 \pm 64 \text{ bar} \tag{1}$$

$\Delta\sigma = 200$ bar was obtained also by Castro *et al.* (2000) for the recent Umbria-Marche earthquake of 26 September 1997. For the attenuation parameters, Rovelli *et al.* (1988) obtained the estimates

$$\kappa_0 = 0.07 \pm 0.02 \text{ sec.} \tag{2}$$

Besides the ones on the attenuation parameters $Q(f)$ and

κ, more studies on the attenuation relationships in the Apennines (Sabetta and Pugliese, 1987; 1996, henceforth SP87 and SP96, respectively) are available. SP87 was the first article in Italy to describe the results of a regression on strong-motion waveforms (accelerograms) to define the attenuation characteristics of the peak horizontal acceleration (PHA) and peak horizontal velocities (PHV). The database used by SP87 contained waveforms generated by events in different tectonic and geological environments. Data were from a compressional region (Friuli) and from three extensional ones; the latter were gathered in two groups (Irpinia and Central Italy-Sicily). SP87 determined the regressions for the logarithms of PHA and PHV with a functional form that did not consider the anelastic energy loss, but described the dependence on distance only in terms of the same geometrical spreading at all distances. Their results are given by the following relationships:

$$\log \text{PHA} = -1.562 + 0.306\text{M} - \log(R^2 + 5.8^2)^{1/2} + 0.169S \quad g \qquad (3)$$

$$\log \text{PHV} = -0.710 + 0.455\text{M} - \log(R^2 + 3.6^2)^{1/2} + 0.133S \quad \text{cm/sec} \qquad (4)$$

To obtain equations (3) and (4), SP87 regressed the largest of the two peaks on the horizontal time histories; M was generally the local magnitude M_L, but M_S was used when both M_L, $M_S \geq 5.5$. The variable R was the closest distance to the surface projection of the fault rupture (in km). SP87 stated that, by chosing R to be the epicentral distance, the final results were very similar, although the standard errors were significantly higher. The variable S takes the values 0 or 1 according to the site geology: in the case of PHA, $S = 0$ for stiff and deep soil sites, $S = 1$ for shallow soil sites; in the case of PHV, $S = 1$ for shallow and deep soil sites, $S = 0$ for stiff ones.

SP96 developed empirical predictive relationships for the vertical and the horizontal components of the response spectra. The database used by both SP87 and SP96 had common components: SP87 used 190 horizontal components from 17 earthquakes recorded in Italy since 1976 ($4.6 \leq M \leq 6.8$); SP96 used 95 accelerograms among the same data set. A multiple regression was carried out by SP96 for 14 different frequencies in the range 0.25–25 Hz; the following functional form was used:

$$\log(y) = a + bM + c\log(R^2 + h^2)^{1/2} + e_1S_1 + e_2S_2 \qquad (5)$$

where S_1 and S_2 refer to the site classification, and take the values 1 for shallow and deep soil sites, and 0 otherwise. As in their previous paper (SP87), SP96 used $c = -1$ (direct-wave geometrical spreading at all distances) and no anelastic attenuation. Table 4 of SP96 provides the values of the other empirical coefficients in their regressions (a, b, e_1, e_2), for each of the chosen frequencies. SP87 and SP96 are currently the reference for the Italian structural engineers.

This study will provide, through an empirical approach somewhat similar to that of SP87 and SP96, a complete attenuation model for the Apennines. The model will reproduce quite successfully the results of SP87 on PHA. Moreover, because we either estimate or physically constrain all the parameters of the attenuation model, and because we use a tool to directly link the Fourier spectra to the peak amplitudes of the ground motion in the time domain, the same model would also describe the attenuation of the Fourier spectra in the Apennines. The approach followed here gives more modern and more flexible results than those provided by the scaling of the PHA or of the response spectra, since it provides the elements for the computation of both.

Evaluation of Regional Scaling Relationships

A possible approach for obtaining regional scaling relationships is to gather a large number of strong-motion recordings and perform regressions on the parameters describing the ground motion (see Campbell and Bozorgnia, 1994, for a worldwide attenuation relationship for the peak horizontal acceleration, or Boore *et al.,* 1993, for a study on data from western North America). On the other hand, our approach to the problem is to use seismograms from the background seismicity, with the great advantage that large amounts of data from microseismic networks become immediately available.

A general form for a predictive relationship is the following:

$$\log a_S(f, r) = \text{EXC}(f, r_{\text{ref}}) + D(r, r_{\text{ref}}, f) + \text{SITE}(f) \qquad (6)$$

whereas $a_s(f, r)$ is the peak amplitude of the ground motion carried by direct S or L_g waves, recorded at the hypocentral distance r. Prior to the regression, seismograms are bandpass-filtered around a set of central frequencies f_{0_i}, and the information about each filtered waveform (peak value, hypocentral distance, event number, station number, pre-event noise level, signal duration, etc.) are stored in a separate table for each central frequency. Alternatively, $a_s(f, r)$ in (6) may indicate, for example, the rms value of the Fourier spectral components, computed between the two corner frequencies that define the bandpass filter centered on f_{0_i} (see Malagnini *et al.,* 2000). A coda normalization technique (Aki, 1980; Frankel *et al.,* 1990) is used to obtain a starting model for $D(r, r_{\text{ref}}, f)$ for the regressions on the peak amplitudes.

The Bandpass Filters

To obtain the filtered time histories around a target frequency f_{0_i}, we apply a high-pass butterworth (8-pole, $f_{c_i} = f_{0_i}/\sqrt{2}$) followed by a low-pass butterworth (8-pole, $f_{c_i} = \sqrt{2}f_{0_i}/$). The term EXC($f$, r_{ref}) in (6) represents (in terms of

peak motion) the seismic source scaled to the reference distance r_{ref}. SITE(f) in (6) indicates the contributions of the site characteristics to the observed peak motion.

The Coda Normalization Technique

The time-domain rms amplitudes of the narrow band-pass-filtered time histories, in windows centered on a total lapse time τ running along the seismic coda (i.e., $\tau \geq 2t_s$), can be represented as:

$$\log[a_C(f, \tau, r)] = \text{EXC}_{\text{Coda}}(f) + C(f, \tau, r) + \text{SITE}_{\text{Coda}}(f) \quad (7)$$

By using the coda normalization method, a normalized function $C_{\text{Norm}}(f, \tau)$ is empirically determined. The coda level for each seismogram at a reference lapse time τ_{ref} is computed, together with the ratio:

$$a_{\text{reduced}}(r, f) = a_S(r, f)/a_C(f, \tau_{\text{ref}}, r) \quad (8)$$

where $a_S(r,f)$ can be the peak amplitude carried by the direct S or the L_g waves, or the Fourier component at frequency f. The essence of this method is that the ratio mathematically eliminates the source and site terms, if the site and excitation effects are identical, and if the coda generation is a linear process:

$$A_{\text{reduced}}(r, f) = \log[a_{\text{reduced}}(r, f)] = D(r, r_{\text{ref}}, f) - C(f, \tau_{\text{ref}}, r) \quad (9)$$

The arbitrariness in the choice of τ_{ref} is removed by forcing $D(r = r_{\text{ref}}, r_{\text{ref}}, f) = 0$. We obtain in this way a first estimate of the scaling law in the region. Since the distribution of the reduced amplitudes is strongly affected by the presence of outliers, a L_1-norm is used in the inversion for the coda-normalized data.

General Regressions

By using (6), we are able to arrange all our observations at frequency f in a large matrix, and simultaneously invert for source, path (attenuation), and site terms. A separate inversion is performed at each sampling frequency, with a starting model for the attenuation term taken from the results of the coda normalization method. $D(r, r_{\text{ref}}, f)$ contains both the effects of geometrical spreading and anelastic attenuation.

A piecewise linear function $D(r, r_{\text{ref}}, f)$ is used for the inversion; following Yazd (1993), we parameterize $D(r, r_{\text{ref}}, f)$ in (6) as a piecewise continuous function with N_{nodes} nodes.

$$D(r, r_{\text{ref}}, f) = \sum_{j=1}^{N_{\text{nodes}}} L_j(r) D_j(f); \qquad D(r = r_{\text{ref}}, r_{\text{ref}}, f) = 0 \quad (10)$$

where $L_j(r)$ is defined as

$$L_j(r) = \begin{cases} \dfrac{r - r_{j-1}}{r_j - r_{j-1}} & \text{if } r_{j-1} \leq r \leq r_j \text{ and } j = 2, 3, \ldots, n \\ \dfrac{r_{j+1} - r}{r_{j+1} - r_j} & \text{if } r_j \leq r \leq r_{j+1} \text{ and } j = 1, 2, \ldots, n-1 \\ 0 & \text{otherwise} \end{cases} \quad (11)$$

$\{D_j(f)\}_1^{N_{\text{nodes}}}$ are node values such that $D(r_j, r_{\text{ref}}, f) = D_j(f)$; the N_{nodes} coefficients $D_j(f)$ are determined by the inversion at each sampling frequency. The presence of a large number of nodes in the parameterization of $D(r, r_{\text{ref}}, f)$ guarantees a great flexibility of the empirical attenuation function, allowing a detailed description of the attenuation phenomena.

A smoothness constraint can be applied during the inversion to $D(r, r_{\text{ref}}, f)$ by requiring:

$$D_{j-1}(f) - 2D_j(f) + D_{j+1}(f) = 0 \quad (12)$$

With an even spatial sampling, the equation above describes a minimum roughness constraint. Throughout this article, the smoothness operator (12) is applied in each regression.

After the inversions are run at the set of central frequencies, $\{f_{0_i}\}$, RVT is used to model the empirical estimate of $D(r, r_{\text{ref}}, f)$. Duration is an input parameter to RVT, and it must be empirically quantified as a function of hypocentral distance at each sampling frequency. The following normalized attenuation function is used for the forward problem:

$$D(r, r_{\text{ref}}, f) = \log g(r) - \log g(r_{\text{ref}}) - \frac{\pi f(r - r_{\text{ref}})}{\beta Q_0 (f/f_{\text{ref}})^{\eta}} \log e; \qquad r_{\text{ref}} = 40 \text{ km}; f_{\text{ref}} = 1.0 \text{ Hz} \quad (13)$$

where β is the shear-wave velocity (3.5 km/sec). The geometrical spreading factor $g(r)$ can be defined on the basis of considerations about the crustal structure of the region of interest: referring to a log–log space, Atkinson (1993) used a trilinear geometrical spreading, whereas other authors (Raoof *et al.,* 1999) required only a bilinear geometrical spreading.

The last step in the processing is the modeling of the inverted excitation terms. A source model calibrated on the region is now necessary. For each sampling frequency, absolute amplitudes are propagated to the reference distance using the attenuation relationship just obtained, and the corresponding duration estimated at the reference distance. A term $\exp(-\pi\kappa_0 f)$ is used to fit the spectral shape of the excitation function at high frequencies. The parameter κ_0 is determined in a trial-and-error procedure. Theoretical excitation terms at the reference hypocentral distance are com-

puted at a set of moment magnitudes and compared to the empirical quantities EXC(f, r_{ref}).

The SITE(f) and EXC(f, r_{ref}) terms defined in (6) are computed in the regression; even though there are more effective methods for investigating these terms, the ones computed here are important to check the stability of the attenuation results. In our computation we do not classify and divide the site terms into specific groups (i.e., stiff and soft soil sites, rock and hard-rock ones). Instead, we reduce the number of free parameters in the regressions by forcing the function $D(r, r_{\text{ref}}, f)$ to be zero at the reference distance,

$$D(r = r_{\text{ref}}, r_{\text{ref}}, f) = 0 \tag{14}$$

This will define an "excitation" term at $r_{\text{ref}} = 40$ km, rather than a "source" term. Another constraint is obtained by forcing

$$\sum_i \text{SITE}(f)_i = 0. \tag{15}$$

The constraint (15) may strongly influence the excitation terms if a common systematic effect is present at all sites. If this situation occurs, the constraint on the site terms forces the common feature into the source terms during the inversion. The excitation term thus represents the network average expected level of motion at the reference distance.

The Data Set

The data set analyzed in this article consists of more than 3,000 three-component seismograms (over 6,000 horizontal time histories), from 446 regional earthquakes. They were recorded by five temporary seismic networks operated by the Istituto Nazionale di Geofisica (ING): three transects across the northern, central and southern Apennines (Amato *et al.,* 1994a, b, 1995a, b, 1998a) and two local networks installed in Umbria (central Italy) to monitor the Massa Martana and the Colfiorito (Umbria-Marche, Amato *et al.,* 1998b) seismic sequences. Most of the recording stations were equipped with broadband instruments.

The five arrays sampled events in different, nonoverlapping periods of time. In order to stabilize the regressions, we introduced recordings taken at two permanent stations of the MedNet network within the time windows of operation of the three transects and of the Colfiorito sequence. In this way, possible tradeoffs due to systematic effects on the recorded amplitudes (instrumental or site-related distortions of the signals) should have been reduced. The two reference stations, AQU and CII, are located near the towns of L'Aquila and Carovilli, respectively, in central and southern Italy. Unfortunately, CII only partially covered the time span of the entire data set.

Accelerograms from two of the main events of the Umbria-Marche sequence ($M_{\text{w}} = 6.0$, and $M_{\text{w}} = 5.7$, recorded by the strong motion stations of the National Accelerometric Network of the Italian Power Company (ENEL), were also included in the data set.

The source-receiver distance distribution for the entire data set is shown in Figures 1 and 2. The y-axes of the two plots display the station names, the x-axes refer to the hypocentral distance. The distance distribution of the data recorded along the three transects is displayed in Figure 1. Figure 2 shows the distribution relative to the data sets of Colfiorito and Massa Martana. Figures 3, 4, 5, and 6 show the maps of the regions of the experiments, with the locations of the recording stations and of the epicentral locations of the events of the data set.

Data Processing

As described in the previous section, each time history of the Italian data set was bandpass-filtered around each of the following sampling frequencies: [f_{0_i} = (0.25, 0.33, 0.4, 0.5, 1.0, 2.0, 3.0, 4.0, and 5.0 Hz)]. The maximum amplitude is then taken from each filtered time history. A second article (Malagnini and Herrmann, 2000) demonstrates that the validity of the results shown in this work can be extended up to 16 Hz.

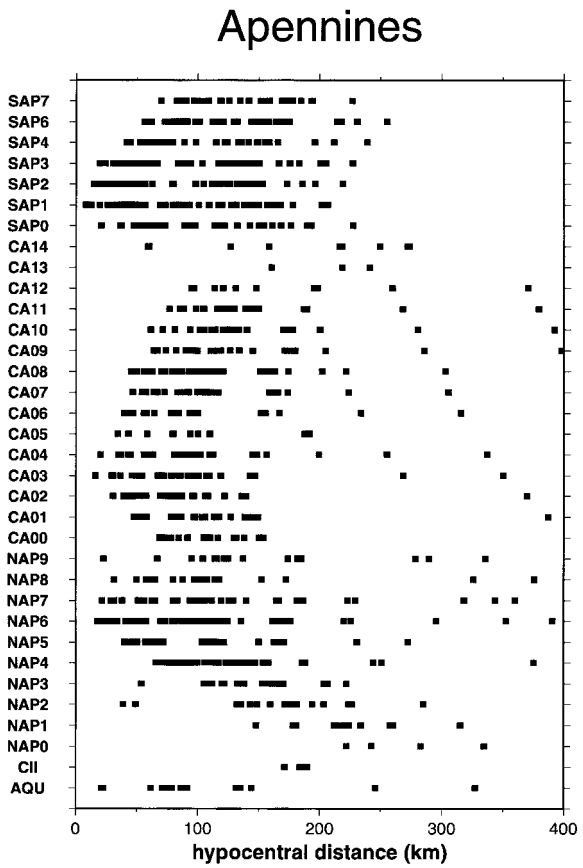

Figure 1. Source-receiver hypocentral distance distribution for the data recorded along the three teleseismic transects.

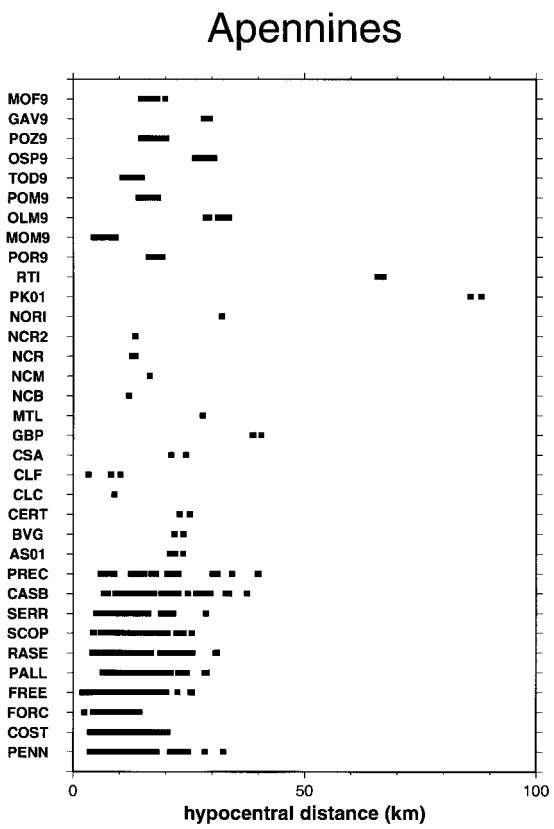

Figure 2. Source-receiver hypocentral distance distributions for the Massa Martana and Colfiorito campaigns.

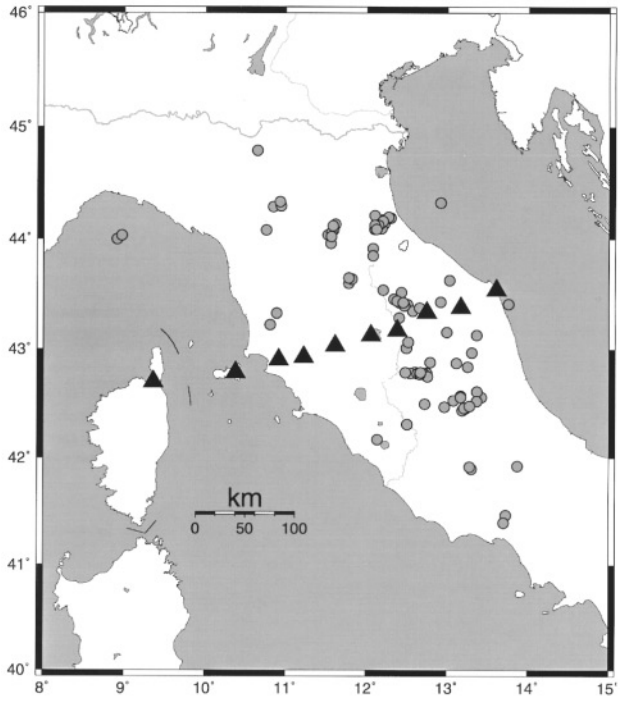

Figure 3. Map of the northern Apennines Teleseismic Transect (1994). Black triangles indicate the positions of the recording stations; gray circles denote the location of the epicenters of the regional events recorded during the experiment. Names of stations go from NAP0 (westermost one, on the Corsica island) to NAP9 (on the Adriatic Sea coastline). NAP stands for Northern Apennines.

Coda Normalization Analysis

Figure 7 shows the estimates of the function $D(r, r_{\text{ref}}, f)$ at 0.5, 1, 2, 3, 4, and 5 Hz, computed over the normalized data. Individual reduced amplitudes are indicated by small dark diamonds. Larger light-gray diamonds indicate the values of $D(r, r_{\text{ref}}, f)$ inverted at the distance nodes.

From a visual inspection of Figure 7 we can see that the distribution of the normalized amplitudes at all frequencies is characterized by the presence of large outliers. For this reason we chose to use an L1-norm minimization of the residuals for this stage of the analysis to avoid biases (the FORTRAN routine is described in Bartels and Conn, 1980).

Duration of Ground Motion

In order to use the RVT to compute the peak values of the filtered time histories, we need to associate each frequency and distance with the corresponding duration of the seismic signal. Following Raoof *et al.* (1999), we estimate the 5%–75% duration of the seismic ground motion for all the available recordings, bandpass-filtered around each one of the sampling frequencies in the following set: 0.25, 0.30, 0.40, 0.5, 1.0, 2.0, 3.0, 4.0, and 5.0 Hz. Figure 8 shows the estimated durations versus the hypocentral distance at some of the indicated frequencies.

Also in this case, an L_1-norm optimization is used to obtain an estimate of the duration as a function of distance at each central frequency. Results of the inversion are shown by the light-gray diamonds in Figure 8. The duration of the seismic signal as a function of distance and frequency is well defined; this functional dependence will be important for the predictive modeling of the ground motion decay through the RVT.

Regional Attenuation

Results of the regressions at a set of sampling frequencies are shown by color lines in Figure 9. Color curves in Figure 9 represent our main result, since they show the empirical estimate of the term $D(r, r_{\text{ref}}, f)$ defined in (6), obtained by a regression on the set of peak values in our data set, each written as in equation (6).

In future applications, the attenuation function will be included either by reading a table with the values plotted in Figure 9, or by defining an analytic expression (an effective attenuation model) that closely matches the empirical curves. In order to provide the attenuation model, we must keep in mind that we deal with peak amplitudes. RVT gives us the ability of predicting the peak amplitude of a time history of duration T, given its Fourier amplitude spectrum.

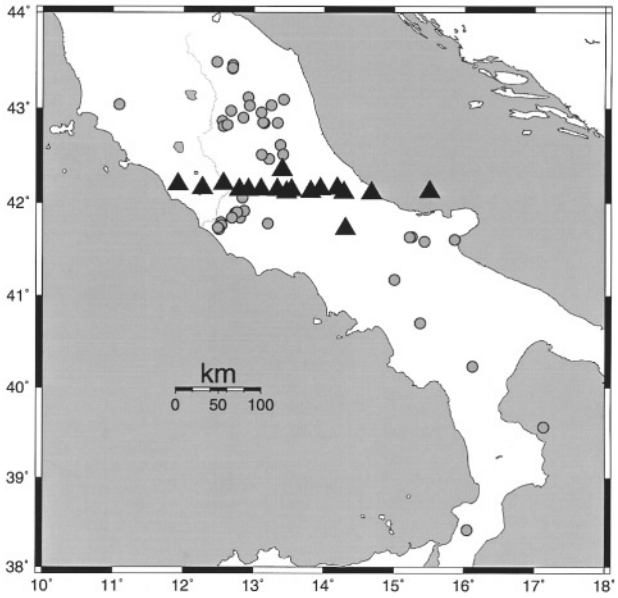

Figure 4. Map describing the central Apennines Teleseismic Transect, deployed in 1995. Black triangles indicate the positions of the recording stations; gray circles denote the epicentral locations of the regional events recorded during the experiment. Names of stations go from CA00 to CA14, from west to east. CA stands for Central Apennines. In the map are also indicated the two MedNet stations used in this study, AQU (north of the transect) and CII (south of it).

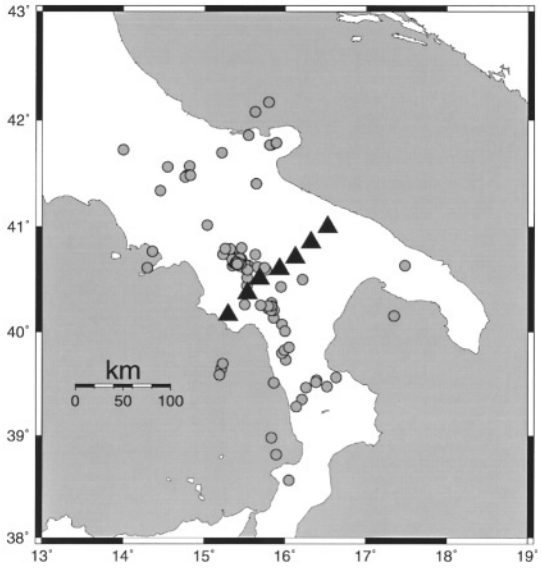

Figure 5. Map of the southern Apennines Teleseismic Transect deployed in 1996. Black triangles indicate the positions of the recording stations; gray circles indicate epicentral locations of the regional events recorded during the experiment. Names of stations go from SAP0 to SAP7, from west to east. SAP stands for Southern Apennines.

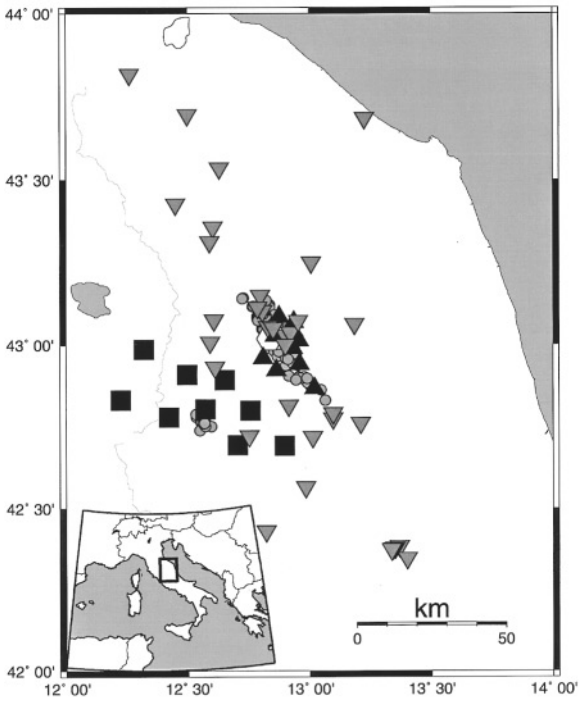

Figure 6. Map of the area struck by the Colfiorito earthquake sequence in September–November 1997, and by the 12 May 1997 event of Massa Martana. The locations of the white hexagons (only one is clearly visible) within the large cloud of gray dots (epicentral locations) show two main shocks of the Colfiorito sequence. The small cloud of epicentral locations located SW of the Colfiorito main events marks the aftershock area of the Massa Martana event. Both sequences were monitored by ING portable arrays deployed in the areas around Massa Martana (black squares indicate the positions of the seismic stations of the portable network, names ending with "9" in Figure 2) and Colfiorito (black triangles represents the ING portable stations (names PREC, CASB, SERR, SCOP, RASE, PALL, FREE, FORC, COST, PENN in Figures 2. Gray inverted triangles indicate the locations of the accelerometers of the National Accelerometric Network run by ENEL, names RTI, PK01, NORI, NCR2, NCR, NCM, NCB, MTL, GBP, CSA, CLF, CLC, CERT, BVG, AS01 in Figure 2).

An earthquake spectral model, like the one by Boore (1983), is used to generate a source spectrum, given a suitable set of the physical parameters that completely describe the source (seismic moment, Brune stress drop, corner frequency, radiation pattern).

In the forward modeling we 'propagate' our spectra to a set of desired distances using the attenuation law. The RVT is used to give a prediction of the peak ground motion as a function of distance, given the estimates of the expected duration and spectral level at each distance. The spectral propagation is obtained by using the functional form:

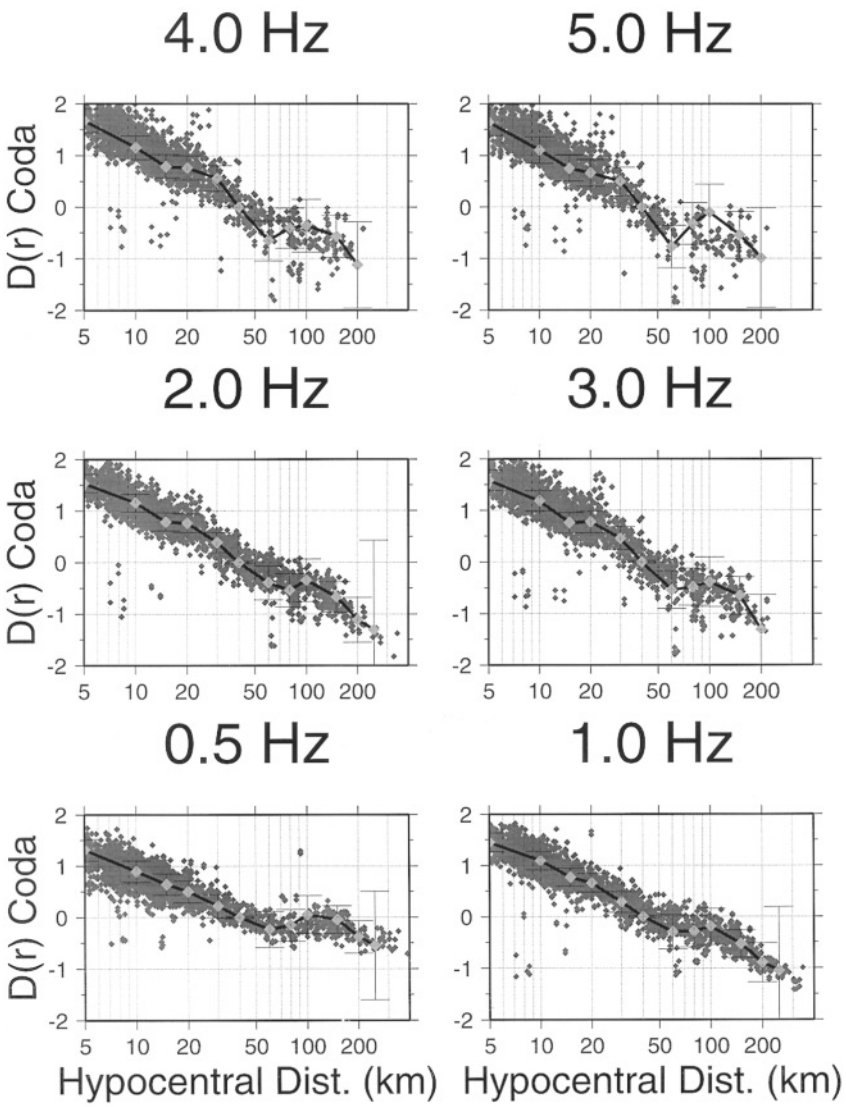

Figure 7. Results of L_1 regressions over the reduced amplitude data (gray small diamonds) at the frequencies indicated above each frame. Light-gray large diamonds represent the coda estimate of $D(r, r_{\text{ref}}, f)$ at the nodal locations. Between each nodal point, the attenuation function is computed by a linear interpolation. The distribution of the raw data is affected by large and numerous outliers. For this reason we chose to use a L_1 minimization algorithm. Note that the attenuation function is normalized to zero at the reference distance of 40 km. Error bars shown in the picture were computed by using a least-squares algorithm, because statistical uncertainties cannot be computed in an L_1 inversion.

$$p(r, f) = \left(g(r) \exp\left[-\frac{\pi f r}{\beta Q(f)} \right] \exp[-\pi \kappa_0 f] \right) \quad (16)$$

where β is the shear-wave velocity (3.5 km/sec). It is worth noticing that, since we now deal with absolute spectral levels, the effect of κ_0 is included in the propagation term (16). The search on the parameter $Q(f)$ and on the geometrical spreading function $g(r)$ is done in a trial-and-error fashion. Remember that we already obtained a quantitative estimate of duration as a function of frequency and distance, to be used by RVT (Figure 8), and so the only free parameters are the ones of the seismic spectra in the region, of the anelastic attenuation, and of the geometrical spreading.

In our modeling, we match the empirical attenuation curves (in color in Figure 9) at all frequencies simultaneously. The attenuation model is defined in equations (13), (18), and (19), and by the empirical estimate of the effective duration. Theoretical curves are the black ones in the background of Figure 9. Note that the plot in the figure are normalized to a r^{-1} geometrical spreading for clarity. Thus the function

$$\log\left(\frac{r}{40}\right) + D(r, r_{\text{ref}}, f) \quad (17)$$

is plotted. The horizontal dashed line in the picture represents a decay proportional to r^{-1}. This representation provides a way of comparing our results with the assumption of constant decay ($\propto r^{-1}$) and of no anelastic attenuation used by SP87 and SP96.

The curves are sensitive to duration, to the functional form of $g(r)$, to the quality factor and its frequency dependence, $Q(f) = Q_0(f/f_{\text{ref}})^{\eta}$. More specifically, the separation between the different curves at a fixed distance gets larger as η decreases; the curves would lie on top of each others if $\eta = 1$. Thus the quality factor chosed by Rovelli *et al.*

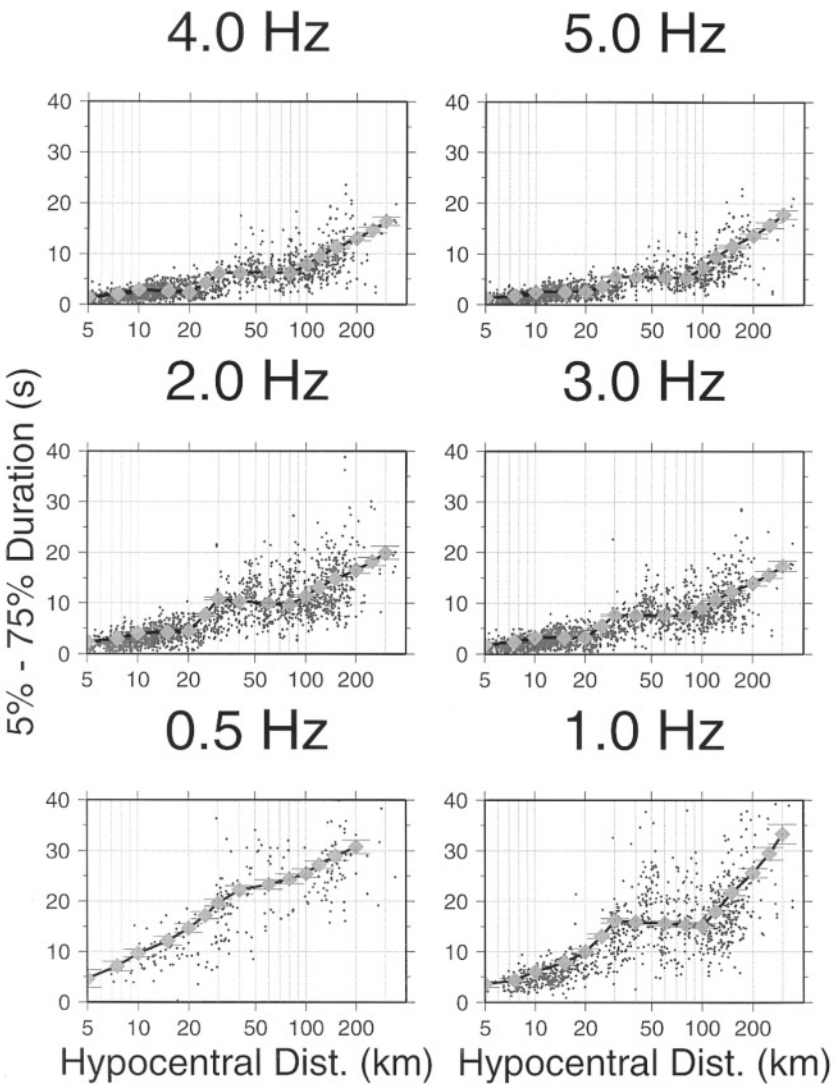

Figure 8. Effective duration of the ground motion, as a function of frequency and hypocentral distance, displayed at a set of sampling frequencies. The *x*-axes of the six frames refer to hypocentral distance (km), and the *y*-axes to duration (sec). Duration is computed as the time window comprising 5–75% of the seismic energy recorded by the specific station. Dark small diamonds indicate individual values of duration. Light gray diamonds indicate the values of duration computed at a set of nodes, by using a L_1 inversion; the associated uncertainties are computed by using a least-squares algorithm.

(1988) would not fit the data. Also, the curves get steeper for lower Q values. Since high frequencies attenuate with distance more severely than low frequencies, $\eta < 1$. Because of the normalization of the curves at the reference distance, Figure 9 is insensitive to the choice of κ_0. We used

$$Q(f) = 130 \left(\frac{f}{f_{\text{ref}}}\right)^{0.10} ; f_{\text{ref}} = 1.0 \text{ Hz} \qquad (18)$$

$$g(r) = \begin{cases} r^{-0.9} & r \le 30 \text{ km} \\ r^{0} & 30 \le r \le 80 \text{ km} \\ r^{-0.5} & r \ge 80 \text{ km} \end{cases} \qquad (19)$$

Site Terms

As a by-product of the final regressions, we obtain source and site terms for each sampled frequency. Site terms for all the available sites for the regressions over the peak values, except for those from the Massa Martana campaign, that are characterized by a strong deviations from the network average, are shown in Figure 10. The Colfiorito site terms agree very well with each other, since almost all stations were deployed on similar geology. As we can see from the figure, site terms from the transects are quite unstable when compared with the ones from Umbria-Marche. This instability is within acceptable bounds, although the comparison strongly suggests that the overall quality of the Colfiorito subset of data is definitely higher. "Quality" in this case is given by several factors, that is, the spatial (distance) and temporal sampling (how many stations were recording data simultaneously) characterizing the data set.

Excitation Terms

The propagation of the rms average spectral component to the reference hypocentral distance is accomplished by multiplying its theoretical estimate by the average crustal path response at the reference hypocentral distance, $p(r =$

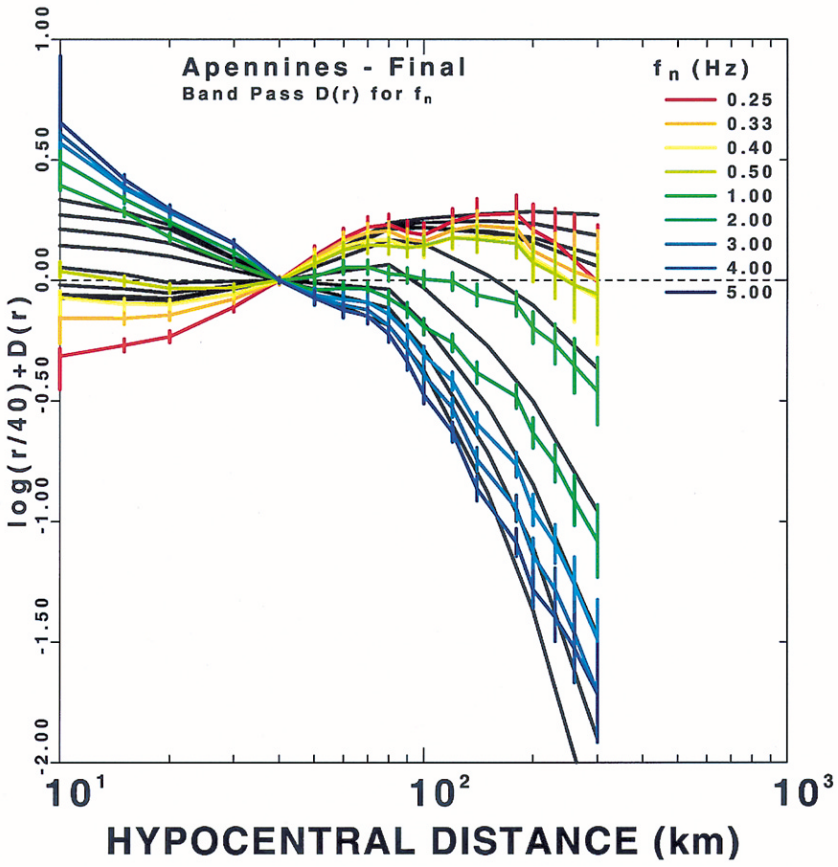

Figure 9. Empirical estimates of $D(r, r_{ref}, f)$, obtained from a set of regressions on the peak values of the filtered ground velocities, carried out at the sampling frequencies of 0.25, 0.33, 0.4, 0.5, 1.0, 2.0, 3.0, 4.0, 5.0 Hz (color lines). The attenuation function is normalized to zero at a reference hypocentral distance of 40 km. The black lines in the background describe our theoretical predictions of the attenuation relationships based on a simple attenuation model and the application of the RVT (see text for details). The figure highlights the deviation from a simple r^{-1} trend (horizontal dashed line).

r_{ref}) (see equation (16)). The attenuation parameter κ_0 describes the high-frequency roll-off of the excitation terms, through the term $\exp(-\pi f \kappa_0)$ in (16) (Anderson and Hough, 1984). Although in its original definition κ_0 was site-specific, in our formulation κ_0 represents a distance-independent regional average of the attenuation in the shallow crust.

Local variations of this parameter are forced into the corresponding site terms. Empirical relationships can be established to couple the value of κ_0 computed at a specific seismic station with the average shear-wave velocity in the weathered layer underneath it: as the average velocity decreases, κ_0 is expected to increase (Atkinson and Boore, 1995). The importance of the effect of the exponential term $\exp[-\pi\kappa_0 f]$ on the spectra has been pointed out by Boore and Joyner (1997) by describing the behavior of a rock site affected by a "generic rock amplification" for different values of κ_0. The same behavior is expected to characterize soil sites, for which we expect higher values of κ_0.

Boore and Joyner (1997) note that the frequency-dependent site response is the result of both structural amplification and anelastic attenuation. Since we do not possess detailed site information, our κ_0 is an effective parameter describing the high-frequency roll-off of source spectra propagated to the site. Our κ_0 thus represents the regional average of the combined effects of generic rock site amplification and anelastic attenuation.

The functional form describing the horizontal velocity spectrum at the reference distance is written as:

$$\mathrm{exc}(f, r_{ref}) = C(2\pi f) M_0 s(f) v(f) p(r_{ref}, f) \qquad (20)$$

where $p(r, f)$ is written in (16),

$$s(f) = \frac{1 - \varepsilon}{1 + (f/f_a)^2} + \frac{\varepsilon}{1 + (f/f_b)^2} \qquad (21)$$

and

$$C = (0.55)(0.707)(2.0)/4\pi\rho\beta^3. \qquad (22)$$

The term $v(f)$ is a generic rock-site amplification term, like the one used by Atkinson and Silva (1997) for California, which was based on that in Boore (1986). In this case we use

$$v(f) = 1.0. \qquad (23)$$

Notice that $\mathrm{EXC}(f, r_{ref})$ in (6) is written as the logarithm of $\mathrm{exc}(f, r_{ref})$ in (20).

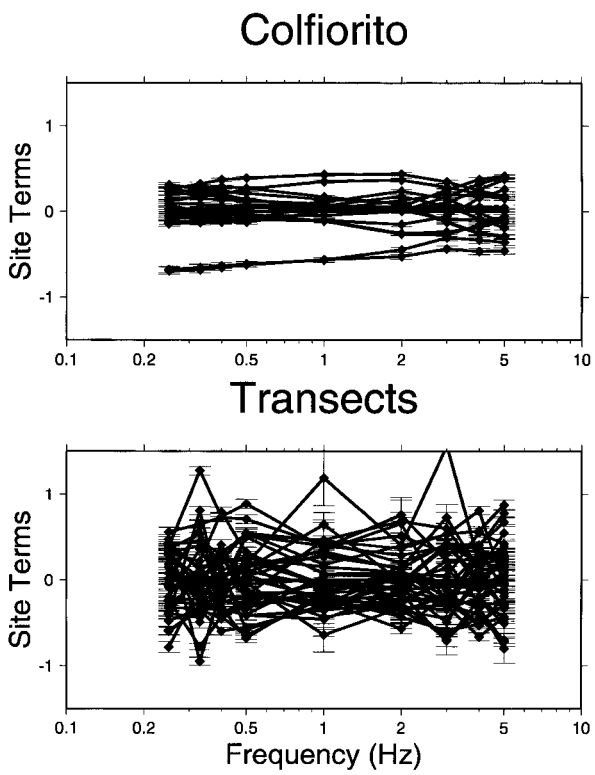

Figure 10. Site terms resulting from the regressions on the entire Italian data set. Although the inversions were simultaneously run on the complete set of seismograms, we show the site terms divided in two groups: sites that recorded the Colfiorito seismic sequence of 1997, labeled "Colfiorito", and sites distributed over the three teleseismic transects, labeled "Transects". The two MedNet site terms are shown in the "Transect" frame.

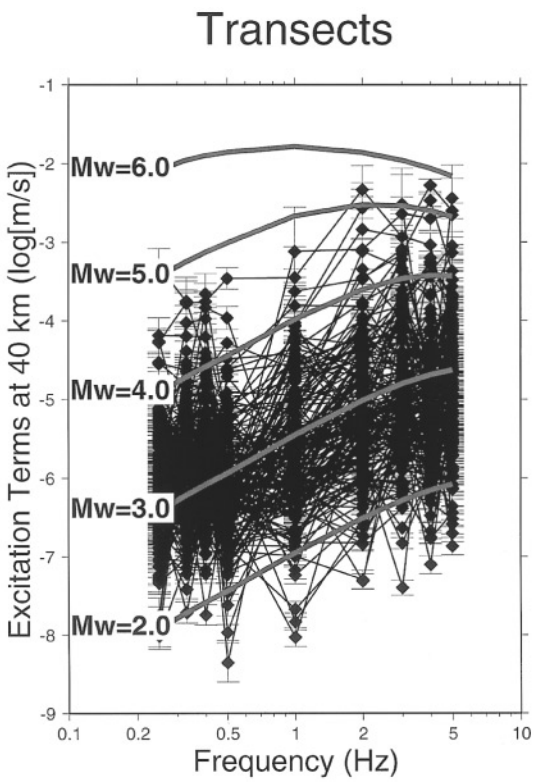

Figure 11. Excitation terms for the events recorded by the three teleseismic transects, compared to predictions obtained by using RVT. Fourier spectra are computed using a Brune source model characterized by the set of parameters shown in Table 1 and attenuated to a reference hypocentral distance $r_{ref} = 40$ km using the regional propagation model defined by equations (16), (18), (19), and (24). RVT is used to compute the peak amplitudes at different frequencies; the effective signal duration at the reference hypocentral distance, needed by the RVT algorithm, is taken from the empirical estimates shown in Figure 8.

Malagnini and Herrmann (2000) used $\kappa_0 = 0.04$ s in their study of the Umbria-Marche region. However, the excitation terms shown in this article, in Figures 11 and 12 are fit by a substantially different high-frequency parameter:

$$\kappa_0 = 0.00 \text{ sec} \tag{24}$$

The significative difference between the values of κ_0 proposed by Malagnini and Herrmann (2000) and the one used here reflects a stronger attenuative properties of rocks in the Umbria-Marche Apennines. This was observed also by Castro *et al.* (1999).

Table 1 gives the numerical values of all the parameters of the spectral model. The value of stress drop indicated in Table 1 is chosen after the indication by Rovelli *et al.* (1988) and Castro *et al.* (2000).

Although the inversion was run on the entire data set, we prefer to show the excitation terms, divided in two groups; Figure 11 displays the ones relative to regional events recorded by the transects and the Massa Martana campaign, whereas Figure 12 shows those relative to events of the Colfiorito (Umbria-Marche) seismic sequence. The empirical excitation terms, independently obtained from the regressions at each frequency, are indicated by the black diamonds; error bars are associated to each of them. Black thin lines link together excitation terms at different frequencies belonging to the same seismic event. Because the regional attenuation function is normalized to a null value at the reference distance of 40 km, the excitation terms represent the expected levels of peak motion at 40 km. Superimposed (thick gray curves) are theoretical predictions computed at various moment magnitudes ($M_w = 2.0, 3.0, 4.0, 5.0, 6.0$). Theoretical excitation terms are produced through RVT and equation (20).

A noticeable difference in the stability of the results exists between the two subsets of inverted excitation terms shown in Figures 11 and 12. We already discussed the difference in the quality of the results characterizing the two subsets (Colfiorito vs. the teleseismic transects). Figure 13

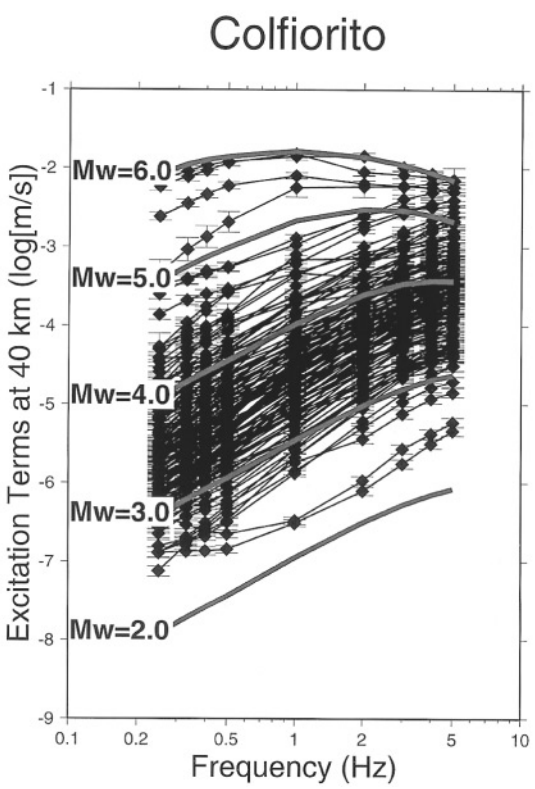

Figure 12. Excitation terms for the events recorded during the Colfiorito (Umbria-Marche) sequence in 1997, compared to predictions obtained by using RVT. Fourier spectra are computed using a Brune source model characterized by the set of parameters shown in Table 1 and attenuated to a reference hypocentral distance $r_{ref} = 40$ km using the regional propagation model defined by equations (16), (18), (19), and (24). RVT is used to compute the peak amplitudes at different frequencies; the effective signal duration at the reference hypocentral distance, needed by the RVT algorithm, is taken from the empirical estimates shown in Figure 8.

Table 1
Parameters of the Brune Spectrum for the Apennines*

ρ	= 2.8 g/cm^3
β	= 3.5 km/sec
$\Delta\sigma$	= 200 bars
f_a	= $4.9 \times 10^6 \beta(\Delta\sigma/M_0)^{1/3}$ Hz
f_b	= f_a Hz
ε	= 1.0
κ_0	= 0.00 sec
$\nu(f)$	= 1

*Spectral parameters used to compute the theoretical excitation terms shown in Figures 11 and 12.

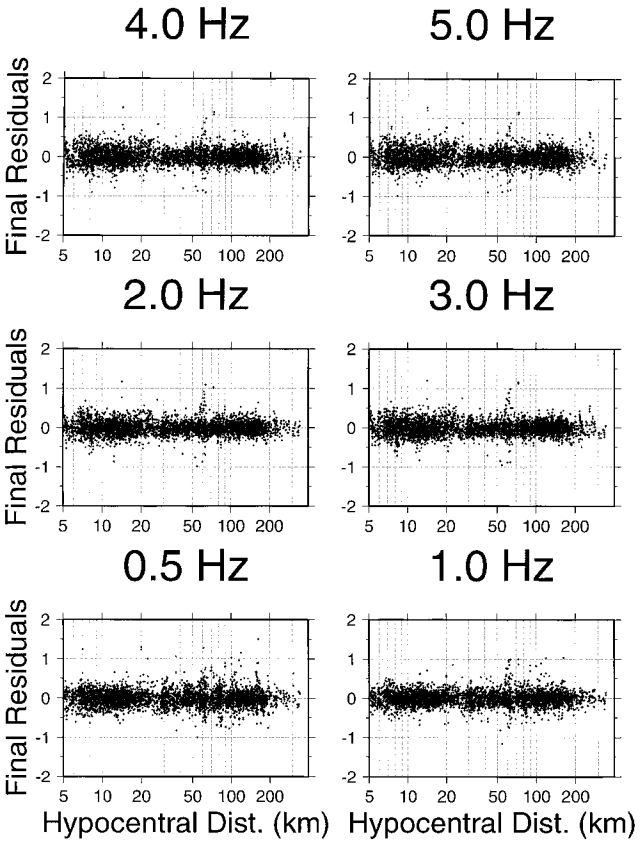

Figure 13. Residuals of the regressions carried out at 0.5, 1.0, 2.0, 3.0, 4.0, and 5.0 Hz.

shows the residuals of the regressions, relative to a set of six sampling frequencies.

Comparison with the results by Rovelli *et al.* (1988)

Figure 14 compares the peak ground velocities at the hypocentral distance of 30 km, which were calculated by using the spectral model described in Table 1 (dashed lines) and the crustal quality factor estimated in this work ($Q(f) = 130f^{0.10}$). Solid lines are obtained by using the same spectral model, but with $\kappa = 0.07$ sec, as estimated by Rovelli *et al.* (1988) and their frequency-dependent quality factor ($Q(f) = 100f$). The distance of 30 km was chosen in order to maintain the same, body-wave-like geometrical spreading to focus the comparison on the attenuation parameters κ_0 and $Q(f)$. Computations were performed for moment magnitudes $M_w = 5.0$ and 6.0.

The absolute differences between the two pairs of peak spectra are not relevant at the hypocentral distance of 30 km (less than a factor of 2). However, since Rovelli *et al.* (1988) used a body-wave geometrical spreading throughout the distance range spanned by their data set, their results may strongly underestimate the expected ground shaking at large hypocentral distances (i.e., beyond 30 km), where the contribution of the geometrical spreading function proposed in this study is much less severe.

The fact that the two pairs of spectra are almost parallel in Figure 14 indicates that the contribution of the parameter $Q_0 = 100$ in the expression proposed by Rovelli *et al.*

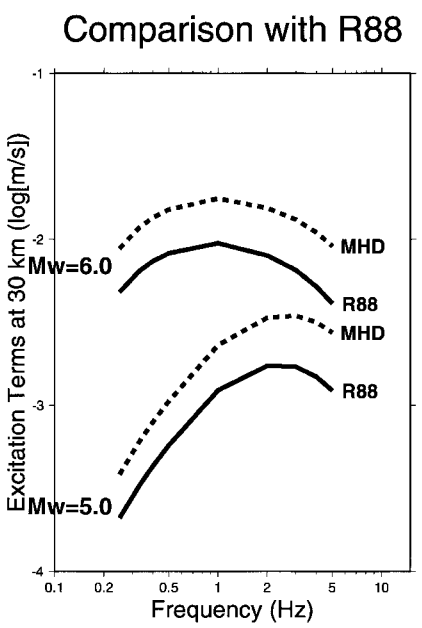

Figure 14. Comparison between the peak velocity spectra computed at a hypocentral distance of 30 km, by using the spectral model described in Table 1 (dashed lines) and the attenuation relationships quantified in this work. Solid lines are obtained by using the same spectral model, but with the attenuation parameters estimated by Rovelli *et al.* (1988). The distance of 30 km was chosen in order to use the same kind of geometrical spreading function, to focus the comparison on the anelastic attenuation parameters. Computations were performed for moment magnitudes $M_w = 5.0$ and 6.0.

(1988), $Q(f) = Q_0 f$, is underestimated. A larger value of this parameter would allow a better agreement between the expected spectra of Figure 14.

Comparison with the coda normalization results

Figure 15 compares the attenuation function obtained from the general regression to its estimate computed by using the coda normalization technique. The figure indicates that the coda normalization represents a good tool for the empirical determination of regional attenuation. What makes it very helpful is that its use is not subject to the availability of well-calibrated recordings. The only requirement is that the station calibration be uniform throughout the data set.

Comparison with Southern California

Ground motion scaling relationships computed in southern California are often used as a standard for other active regions of the world. Our results can be compared with those computed for southern California by Raoof *et al.* (1999), and we feel that these may be inappropriate for the Apennines. Other than some minor differences of the two data sets, the procedure applied in the two cases is virtually identical. Figure 16 compares the Italian $D(r, r_{ref}, f)$ to the results from southern California. The attenuation functions from the two regions are very similar at 0.5 and 1.0 Hz, but at higher frequency the differences are significant, with stronger attenuation in Italy. Given this comparison, the use of empirical relationships developed in southern California for applications in the Apennines must be discouraged, even for the estimate of the magnitude of an earthquake based on the duration of the ground motion. The reason for this is discussed in a later section. In addition, our estimate of $\kappa_0 = 0.00$ sec is much lower than the one estimated in southern California by Raoof *et al.* (1999).

Peak Ground Motion

RVT is used to compute the expected PHA and the PHV, given the seismic spectra described in Table 1 and our estimate of the crustal attenuation, $D(r, r_{ref}, f)$, and of the duration function. The computer code (Boore, 1996) uses a linear relationship with zero offset to describe the increase of duration with hypocentral distance, and we input an average slope value of 0.06 sec/km based on our duration analysis.

Our estimates of PHA for a moment magnitudes $M_w = 5.0$, 6.0, and 7.0, are labeled as M2000 in Figure 17. The Figure compares our results with the regressions of Sabetta and Pugliese (1987), labeled as SP87. The thick segments on the SP87 lines represents the range of distances where strong-motion data were available for the SP87 regressions. It is encouraging to see that the agreement at $M_w = 7$ between our estimates and their results is good on average, since SP87 could use data in a wide distance range, up to 200 km away from the earthquake and given their simple geometrical spreading. At lower magnitudes the two sets of curves are still in a fairly close agreement within the distance range covered by data in the SP87 study, although their linear curves significantly diverge from ours at large distances.

The PHVs, on the other hand, show a different behavior (Figure 18). For large magnitudes ($M \sim 7$) the SP87 results and our estimates are in fair good agreement at short distances ($r \leq 30$ km), but beyond the first crossover distance of our geometrical spreading, our estimates are significantly higher than the regression curves of SP87. For smaller magnitudes ($M = 5, 6$), the two sets of curves are in better agreement, at least within the distance ranges covered by data in the work of SP87.

The differences between our theoretical predictions and the empirical curves may be due to two factors: the source spectrum model used for the predictions and the magnitudes used for the empirical regressions. The magnitude problem is discussed in the next section. The source spectrum model of large earthquakes in the Apennines is probably inadequate for reproducing the lower frequencies that control the PHV. A two-corner frequency source model might represent a better choice for large earthquakes in the region, since such a spectral model would be characterized by lower peak amplitudes at intermediate frequencies. Recall that velocity spectra are dominated by intermediate frequencies.

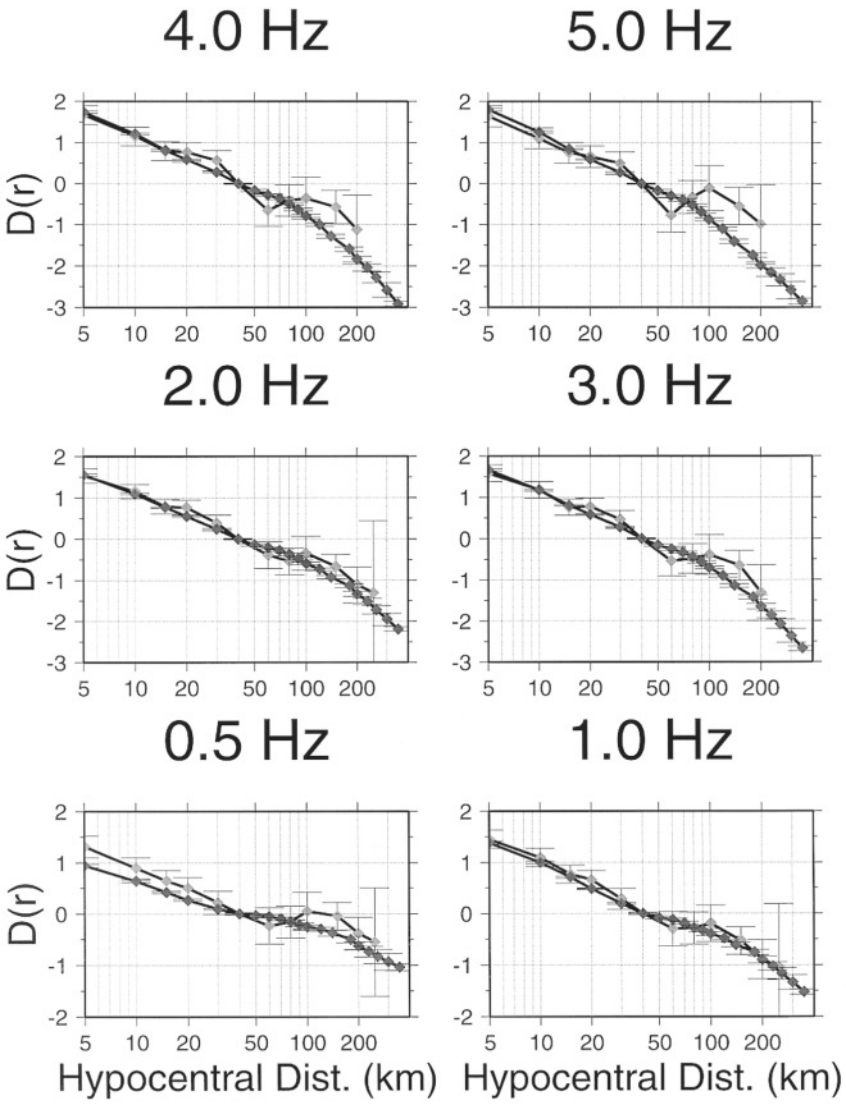

Figure 15. Comparison between the attenuation function obtained from the regressions on the logarithms of the peak amplitudes (dark-gray diamonds), and its initial estimate obtained with the coda normalization technique (light-gray diamonds). The six frames in this picture show the comparison at the frequencies of: 0.5, 1.0, 2.0, 3.0, 4.0, and 5.0 Hz.

Magnitude Estimates

Since the beginning of our investigation, we noticed a systematic divergence between the duration magnitudes estimated routinely at ING and the corresponding amplitude levels of our excitation terms. For example, the upper limit for the magnitude distribution of the 1996 data used in this article was $M_{\mathrm{dING}} = 3.8$ for an event of 27 April 1996 at 00:38 UT, which was listed as a $m_{\mathrm{b}} = 4.6$ in the NEIC catalog. For this event, our amplitude level agrees with the NEIC amplitude (Figure 19).

It is well known that the duration magnitudes are systematically lower than the moment magnitudes above a certain threshold, when durations are estimated from the output of short-period seismometers. The shift of the corner frequency for increasing earthquake size, coupled with the instrument response of short-period seismometers, leads to saturation for M_{d} for large earthquakes (Herrmann, 1975). Giardini *et al.* (1997) calibrated regression curves commonly used for earthquakes within the Mediterranean region, and concluded that the duration magnitude M_{D} used by most seismic networks requires accurate station calibration and should be restricted only to events with low seismic moment.

For the events in our data set, we noticed that M_{dING} seriously underestimates the moment magnitudes above $M_{\mathrm{w}} \simeq 3.4$. Figures 19 and 20 illustrate our attempt to test our capability of providing correct absolute values of the ground shaking at the reference distance of 40 km. It must be clear that what follows does not provide a new tool for the computation of the magnitude along the Apennines, but rather highlights the discrepancy between the magnitudes listed in the Italian earthquake catalog and the corresponding estimates of M_{w} or m_{b}. Four earthquakes in our data set had independent estimates of magnitude that could be compared with the corresponding M_{dING} values listed in the ING cata-

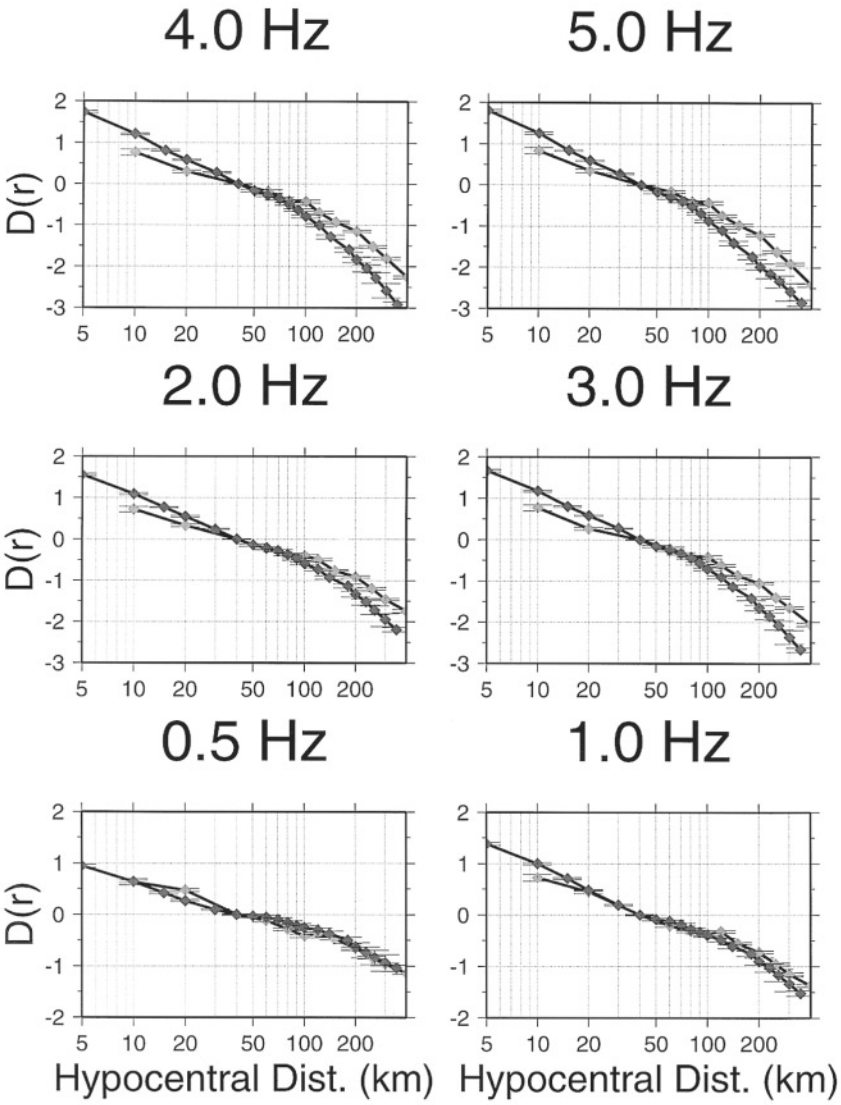

Figure 16. Comparison between the attenuation function computed for the Apennines (dark-gray diamonds) and the one provided by Raoof *et al.* (1999) for southern California (light-gray diamonds). This comparison is important because southern California is often used as a reference standard for strong ground motion studies. From this picture we see that the attenuation in the two regions is quite similar at 0.5 and 1.0 Hz, whereas at higher frequencies there are substantially different behaviors.

log. The comparison is made in Figure 19, where the two upper dark-gray lines show the excitation terms of two events recorded during the Colfiorito seismic sequence, the first on 26 September 1997, at 00:33 UT (M_w = 5.67, Ekström *et al.,* 1998), the second at 9:40 UT the same day (M_w = 6.00, Ekström *et al.,* 1998). The third dark curve in the picture is for an event that occurred in the Colfiorito area on 27 September 1997 at 08:08 UT (M_w = 4.35, Ekström *et al.,* 1998). The light-gray line in Figure 19 corresponds to an event that occurred on 27 April 1996 at 00:38 UT, for which NEIC provided a magnitude m_b = 4.6. For this event M_{dING} = 3.8. The duration magnitudes provided by ING are indicated in light and dark gray on the right side of Figures 19, according to the level of gray of the corresponding line. The values of M_w indicated in dark and light gray on the left side of the picture are the ones used to compute our theoretical predictions (smooth gray lines).

Figure 20 shows the computed excitation terms corresponding to two earthquakes, which occurred on 16 July 1996 at 12:46 UT and on 19 July 1996 at 01:20 UT. We obtained a good fit for our excitation amplitudes at 40 km (black lines), by using M_w = 3.4 (M_{dING} = 3.4). Figure 20 illustrates that $M_{dING} \sim M_w$, for $M_{dING} \sim 3.4$, whereas Figure 19 illustrates how M_{dING} underestimates true sizes for larger events.

The use of duration as a measure of magnitude is described by many authors (Biszticsany, 1958; Sole'vev, 1965; Tsumura, 1967; Lee *et al.,* 1972; Crosson, 1972, Real and Teng, 1973). A general formulation for the duration magnitude is the following:

$$M_d = p + q \log \tau + s\Delta \qquad (25)$$

where τ is the duration of the seismic signal, from the onset of *P* waves, and Δ is the epicentral distance. *p*, *q*, and *s* are parameters to be empirically estimated in the region of interest. Although quantitatively defined and automatically computed, the durations used at ING to calculate the mag-

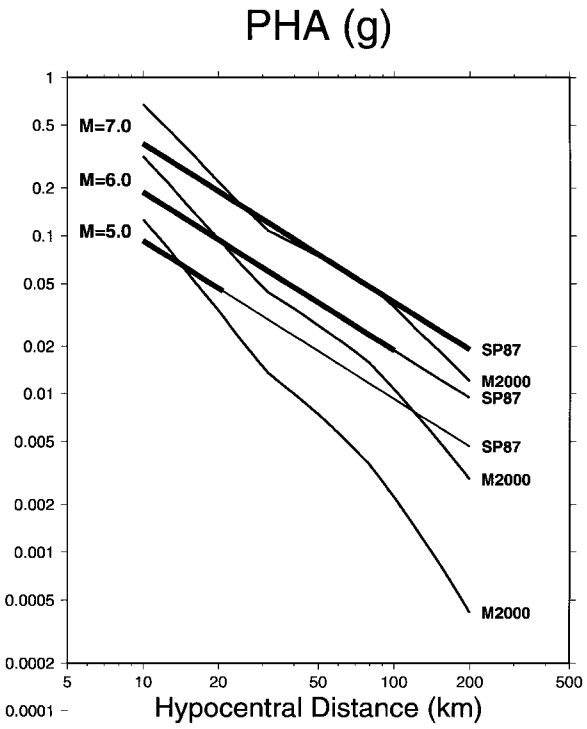

Figure 17. Estimates of peak horizontal acceleration obtained, through RVT, using the attenuation parameters obtained in this study and the spectral model indicated in Table 1 (curves marked M2000). These are compared with the results of the regressions by SP87, summarized by equation (3); curves are labeled SP87. The ranges of distance actually covered by the data set of SP87 at different magnitudes are indicated on each line by a thick segment. The SP87 curves have been extrapolated to large distances by using equation (3).

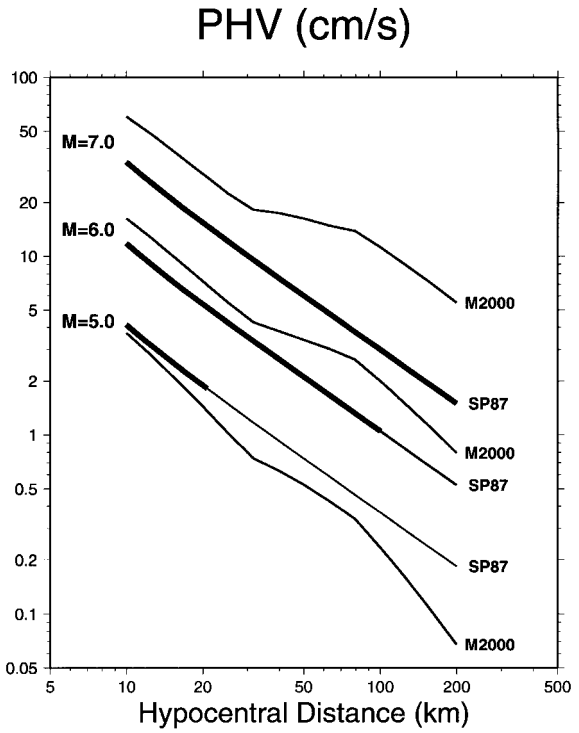

Figure 18. Estimates of peak horizontal velocity based on the attenuation function obtained through RVT, using the attenuation parameters obtained in this study and the spectral model indicated in Table 1 (curves marked M2000). These are compared with the results of the regressions by SP87, summarized by equation (4); curves are labeled SP87. The ranges of distance actually covered by the data set of SP87 at different magnitudes are indicated on each line by a thick segment. The SP87 curves have been extrapolated to large distances by using equation (4).

nitudes for the seismic catalog are always estimated by the operator on duty, directly from the seismic signal.

Herrmann (1975) noted that for small earthquakes, the q parameter in (25) is related to the coda envelope shape, which can be written as

$$a(t) = A_0 \left(\frac{\tau}{t_s - t_p} \right)^{-\delta} \tag{26}$$

where

$$\tau = t - t_p. \tag{27}$$

A_0 is proportional to the seismic moment ($A_0 \propto M_0$), especially if small earthquakes are studied, for which the source corner frequency is within, or greater than, the sensor bandpass. If the duration τ is defined as

$$\tau = t_{\text{noise}} - t_p \tag{28}$$

and t_{noise} is such that

$$a(t_{\text{noise}}) = C \cdot a_{\text{noise}} \tag{29}$$

where a_{noise} is the noise amplitude, and C is an arbitrary constant, larger than 1 ($C = 2$ could be a good choice for observations), then

$$a(t_{\text{noise}}) \propto M_0 \left(\frac{\tau}{t_s - t_p} \right)^{-\delta} \tag{30}$$

taking the logarithms,

$$\log a(t_{\text{noise}}) = \log M_0 - \delta \log \tau + f(r) + \text{const} \tag{31}$$

where $f(r) = \delta \log(t_s - t_p)$ is a function of the hypocentral distance. If we want to use τ to estimate the magnitude of an event, we can use the relationship

$$M_w = \frac{1}{1.5} \log M_0 + \text{const.} \tag{32}$$

(Hanks and Kanamori, 1979) which presumably holds also

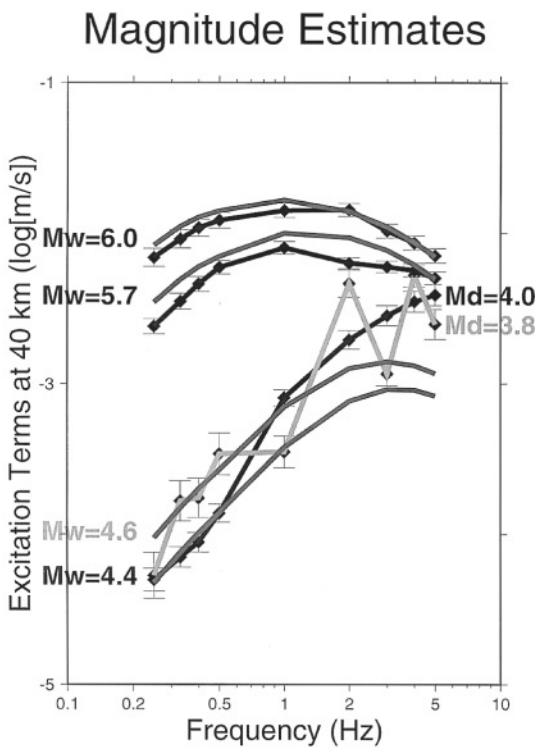

Figure 19. Excitation terms of events for which we have some independent magnitude estimates (the NEIC catalog, number in light gray on the left side of the picture, and Ekström *et al.,* 1998, number in dark gray on the left side of the picture). The corresponding theoretical excitation terms estimated through RVT are plotted (gray lines). The cited, independent moment-magnitude estimates are indicated on the left side. Dark lines refer to the empirical excitation terms obtained from the regressions, relative to events of the Colfiorito seismic sequence; the light-gray line refers to the empirical excitation term relative to an event recorded by the 1996 southern Apennies teleseismic transect. On the right side of the picture, in light and dark gray, are indicated the values of M_{dING} for the two low-magnitude events. Notice the substantial differences between the corresponding values of M_{w} and M_{dING}.

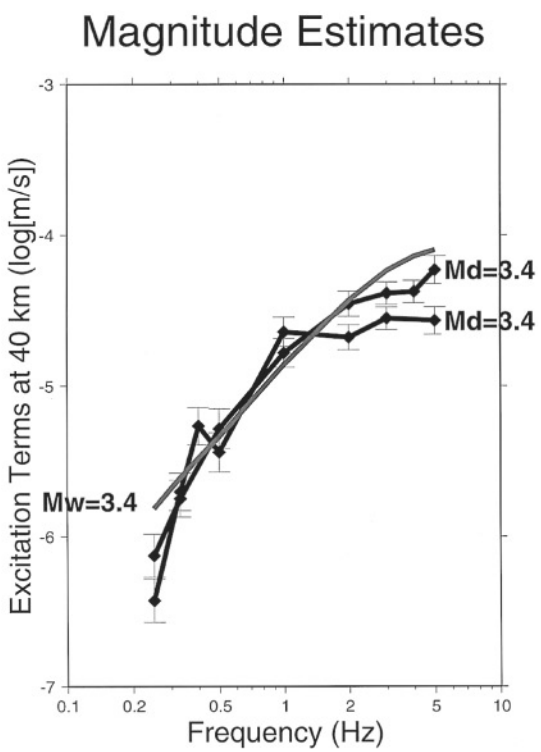

Figure 20. The figure shows two empirical excitation terms obtained from the regressions on the peak amplitudes (black lines), with the indication of their duration magnitudes ($M_{\mathrm{dING}} = 3.4$) on the right side of the picture. The events were recorded by the 1996 southern Apennines teleseismic transect. The gray curve represents a theoretical prediction of the observed excitation terms, for a moment magnitude $M_{\mathrm{w}} = 3.4$.

for events in the Apennines, and write

$$M_d = q \log \tau + \text{const.} \tag{33}$$

where

$$q = \frac{\delta}{1.5}. \tag{34}$$

The coefficient 1.5 derives from the empirical relationships defined by Gutenberg and Richter to relate the seismic energy to the magnitude M_{s} (see Lay and Wallace, 1995, p. 384).

For the Italian region, Console *et al.* (1988) proposed

$$M_{d\mathrm{ING}} = -0.87 + 2 \log(\tau + 0.08236\Delta). \tag{35}$$

Lee *et al.* (1972) used the following relationship for California:

$$M_{d\mathrm{ING}} = -0.87 + 2[\log \tau + 0.00175\Delta]. \tag{36}$$

Figure 21 suggests that the choice of q ($= 2.0$, corresponding to $\delta = 3.0$) made by Console *et al.* (1988) in the formula for the definition of the duration magnitude is inadequate for the Italian region. The upper frame shows a horizontal time history from the event of 27 April 1996 at 00:38 UT ($m_{\mathrm{b}} = 4.6$). The dotted and dashed lines describe the coda decay function for $\delta = 3.0$ and $\delta = 4.0$, respectively. In the lower frame is shown a log–log plot of the absolute values of the time history as a function of time, together with lines proportional to $t^{-3.0}$ (dotted), and $t^{-4.0}$ (dashed).

Although a proper reevaluation of the duration-magnitude relationship for the Italian region would require a regression on a large data set, it is clear that the formula of Console *et al.* (1988) should be reconsidered in the light of this simple example. The new parameter might be:

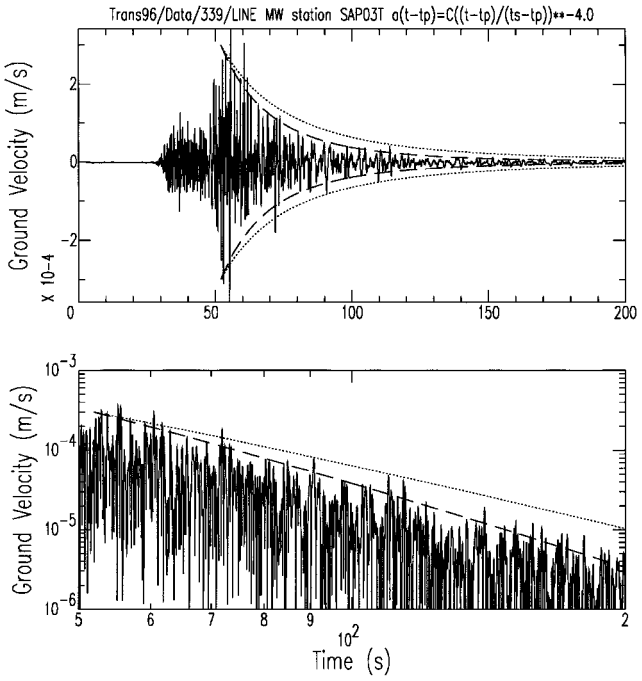

Figure 21. (Upper frame) Transverse component of ground motion recorded by station SAP3 (southern Apennines Transect, 1996) during the event that occurred on 27 April 1996 at 00:38 UT ($m_b = 4.6$). The envelope of the seismic signal after the *S*-wave arrival is outlined by the dashed curves corresponding to a normalized amplitude decay with time proportional to $t^{-4.0}$ (see equation (26)). The dotted curves represent a normalized decay proportional to t^{-3}, as indirectly assumed by Console *et al.* (1988). (Lower frame) The absolute values of the horizontal time history are plotted in a log log fashion. Again, the dashed and dotted lines represent the $t^{-4.0}$ and the t^{-3} normalized decays with time (time scales of the two frames are different).

$$q = \frac{\delta}{1.5} = \frac{4.0}{1.5} \simeq 2.67 \qquad (37)$$

This is another example of the effect of different wave propagation in the Apennines and southern California, since the parameters of the formula to be used to estimate the duration magnitude are determined by the regional attenuation characteristic, which we showed to be significantly different at high frequency.

Conclusions

We determined empirical regional attenuation relationships for the peak amplitudes of *S* and *Lg* waves in the Apennines. This result was achieved by performing regressions over a large number of time histories (over 6000 horizontal waveforms), which have been collected in about five years along the entire Apennines fold-and-thrust belt. Most of the data set consists of broadband seismograms from local portable networks, although a small part of it ($\sim$ 200 horizontal-component waveforms) comes from accelerometric recordings collected during the strongest events of the recent Colfiorito sequence (largest magnitudes included in the data set: $M_w = 6.0$ and $M_w = 5.7$).

Regressions were performed over the peak amplitudes of bandpass-filtered versions of the original seismograms. Filtering was carried out over a discrete set of sampling frequencies between 0.25 and 5.0 Hz.

We model the attenuation of the logarithm of the *S*- or *Lg*-wave peak amplitudes, normalized to zero at an arbitrary hypocentral distance r_{ref}, using equation (13) and the following geometrical spreading function ($g(r)$) and crustal quality factor ($Q(f)$):

$$g(r) = \begin{cases} r^{-0.9} & r \le 30 \text{ km} \\ r^{0} & 30 \le r \le 80 \text{ km} \\ r^{-0.5} & r \ge 80 \text{ km} \end{cases}$$

$$Q(f) = 130(f/f_{ref})^{0.10},\ f_{ref} = 1.0 \text{ Hz}.$$

As we demonstrate in a different article (Malagnini and Herrmann, 2000), this frequency dependence is valid in a broader frequency range (0.25–16.0 Hz) than the one explored in this study (0.25–5.0 Hz). Seismic spectra at $r = r_{ref}$ are reproduced using a Brune spectral model characterized by a stress drop $\Delta\sigma = 200$ bars, and a parameter

$$\kappa_0 = 0.00 \text{ sec}.$$

This estimate of κ_0 is significantly different from that of Malagnini and Herrmann (2000) in the Umbria-Marche Apennines ($\kappa_0 = 0.04$ sec). This is explained, in agreement with Castro *et al.* (1999), by a stronger attenuation properties affecting the earthquake recordings in the Umbria-Marche Apennines.

Our estimate of the attenuation parameters for the Apennines apparently contrasts with the results of Rovelli *et al.* (1988). We show that this disagreement is only apparent at short hypocentral distances (less than 30 km); at larger distances, because of a different geometrical spreading, our predictions are substantially higher than the ones obtained by using a constant, body-wave geometrical spreading and the anelastic parameters estimated by Rovelli *et al.* (1988).

The effective duration of the ground motion to be used in the Apennines is obtained by analyzing small earthquakes. We estimate the duration resulting only from dispersion, representing the crustal response to a space-time Dirac-δ excitation. Duration is estimated as a function of hypocentral distance and frequency. Duration of an earthquake rupturing an extended fault can be obtained by translating upward the curves of Figure 8 by a quantity related to the rupture time, after taking into account the related saturation phenomena.

We showed that the attenuation function for southern California (a region historically viewed as the reference standard for studies on ground motion in active regions) is sub-

stantially different from the Italian attenuation for frequencies above 1 Hz. For predicting the ground motion in the Apennines, the Italian seismological community must therefore use only tools calibrated over the Italian region. In the last section of this article we demonstrate that the duration–magnitude relationship given by Console *et al.* (1988) may be inadequate to describe the actual source sizes away from $M_w \approx 3.4$.

An important implication of this work, together with the one by Malagnini and Herrmann (2000), is that because of the low-Q at all frequencies, high-frequency (1–20 Hz) seismic hazard in the Apennines may be dominated by the local seismicity. For the future we are planning to perform similar studies over sets of data from the Western and Eastern Alps and from Sicily. This complex effort will eventually allow the production of modern hazard maps for the entire Italian territory.

Acknowledgments

The authors wish to thank Prof. Enzo Boschi, who strongly supported this research. Without his help we would not have accomplished these results. Many people contributed to this effort with comments and discussions. We wish to thank Chuck Ammon, Aybige Akinci, Roberto Ortega, Brian Mitchell, David Kirschner, Sean Morrissey, Barbara Palombo, Antonio Rovelli, and David Crossley (mentioned in a random order) for help and for the strong and constructive criticism they gave us. We thank Martin Chapman and two anonymous referees for providing valuable suggestions that significantly improved the readability of the article. Alessandro Amato and his group at ING organized the data from the teleseismic transects, Andrea Morelli kindly provided the MedNet data for earthquakes recorded by the transects and by the temporary network that ING deployed in the Umbria-Marche region. The Italian power company (ENEL) provided the strong-motion recordings. Finally, we thank all the people who went in the field during the Massa Martana and Colfiorito campaigns and contributed to the storage and preliminary analysis of the collected data: Riccardo Azzara, Pio Lucente, Lucia Margheriti, Concetta Nostro, Claudio Chiarabba, Alessandro Amato, Massimo Cocco, Giulio Selvaggi, Gianni Cimini, and many more. Their great effort made this work possible. The three teleseismic transects were funded by the European Community (Contract EV5V-0464). Other campaigns were entirely funded by ING. This work was partially carried out in the framework of the project "Probable Earthquakes in Italy from Year 2000 to 2030," funded by the Gruppo Nazionale per la Difesa dai Terremoti.

References

Aki, K. (1980). Attenuation of shear waves in the lithosphere for frequencies from 0.05 to 25 Hz, *Phys. Earth Planet. Inter.* **21,** 50–60.

Aki, K., and B. Chouet (1975). Origin of the coda waves: source, attenuation and scattering effects, *J. Geophys. Res.* **80,** 3322–3342.

Amato, A., R. Azzara, A. Basili, C. Chiarabba, G. B. Cimini, M. Di Bona, and G. Selvaggi (1994a). Geo-ModAp: a teleseismic transect across the Northern Apennines (Italy), *EOS,* 1994 Fall meeting, S01–48.

Amato, A., R. Azzara, A. Basili, C. Chiarabba, G. B. Cimini, M. Di Bona, L. Margheriti, C. Nostro, and G. Selvaggi (1994b). The Northern Apennines Teleseismic Transect (1994), Istituto Nazionale di Geofisica, technical report.

Amato, A., R. Azzara, A. Basili, C. Chiarabba, G. B. Cimini, M. Di Bona, F. P. Lucente, L. Margheriti, C. Nostro, G. Selvaggi (1995a). The Central Apennines Teleseismic Transect (1995), Istituto Nazionale di Geofisica, technical report.

Amato, A., C. Chiarabba, G. B. Cimini, M. Di Bona, L. Margheriti, C. Nostro, and G. Selvagi (1995b). Deep structure beneath the Northern Apennines (Italy) from passive seismological studies, IUGG XXI Assembly, 2–14 July 1995.

Amato, A., L. Margheriti, R. Azzara, A. Basili, C. Chiarabba, M. G. Ciaccio, G. B. Cimini, M. Di Bona, A. Frepoli, F. P. Lucente, C. Nostro, and G. Selvaggi (1998a). Passive seismology and deep structure in central Italy, *Pure Appl. Geophys.* **151,** 479–493.

Amato, A., R. Azzara, C. Chiarabba, G. B. Cimini, M. Cocco, M. Di Bona, L. Margheriti, S. Mazza, F. Mele, G. Selvaggi, A. Basili, E. Boschi, F. Courboulex, A. Deschamps, S. Gaffet, G. Bittarelli, L. Chiaraluce, D. Piccinini, and M. Ripepe (1998b). The 1997 Umbria-Marche, Italy, earthquake sequence: a first look at the main shocks and aftershocks, *Geophys. Res. Lett.* **25,** 2861–2864.

Anderson, J. G., and S. E. Hough (1984). A model for the shape of the Fourier amplitude spectrum of acceleration at high frequencies, *Bull. Seism. Soc. Am.* **74,** 1969–1993.

Atkinson, G. M. (1993). Earthquake source spectra and attenuation in southeastern Canada, *Ph.D. Thesis,* University of Western Ontario, London, Ontario.

Atkinson, G. M., and D. M. Boore (1995). Ground-motion relations for eastern North America, *Bull. Seism. Soc. Am.* **85,** 17–30.

Atkinson, G. M., and W. J. Silva (1997). An empirical study on earthquake source spectra, *Bull. Seism. Soc. Am.* **76,** 43–64.

Bartels, R. H., and A. R. Conn (1980). Overdetermined systems of linear equations in the L1 sense, with or without linear constraints, *ACM TOMS* **6,** 609–614.

Bisztricsany, E. (1958). A new method for the determination of the magnitude of earthquakes, *Geofiz. Kozlemen* **7,** 69–96.

Boore, D. M. (1983). Stochastic simulation of high-frequency ground motion based on seismological models of the radiated spectra, *Bull. Seism. Soc. Am.* **73,** 1865–1894.

Boore, D. M. (1986). Short-period *P*- and *S*-wave radiation from large earthquakes: implication for spectral scaling relations, *Bull. Seism. Soc. Am.* **76,** 43–64.

Boore, D. M. (1996). SMSIM: Fortran programs for simulating ground motion from earthquakes: version 1.0, *U.S. Geol. Surv. Open-File Rept. 96-80-A,* 73 pp.

Boore, D. M., and W. B. Joyner (1997). Site amplification for generic rock sites, *Bull. Seism. Soc. Am.* **87,** 327–341.

Boore, D. M., W. B. Joyner, and T. E. Fumal (1993). Estimation of response spectra and peak acceleration from western North America earthquakes: An interim report, *U.S. Geol. Surv. Open-file Rept. 93-509,* 72 pp.

Brune, J. N. (1970). Tectonic stress and the spectra of seismic shear waves from earthquakes, *J. Geophys. Res.* **75,** 4997–5009.

Brune, J. N. (1971). Correction, *J. Geophys. Res.* **76,** 5002.

Campbell, K. W., and Y. Bozorgnia (1994). Near-source attenuation of peak horizontal acceleration from worldwide accelerograms recorded from 1957 to 1993, in *Proc. Fifth U.S. National Conference on Earthquake Engineering, E.E.R.I.,* Berkeley, California, Vol. 1, 283–292.

Cartwright, D. E., and M. S. Longuet-Higgins (1956). The statistical distribution of the maxima of a random function, *Proc. R. Soc. London,* Ser. A237, 212–232.

Castro, R. R., A. Rovelli, M. Cocco, F. Pacor, and M. Di Bona (2000). Stochastic simulation of strong-motion records from the September 26, 1997 ($M_w = 6$) Umbria-Marche (Central Italy) earthquake, *Bull. Seism. Soc. Am.* (submitted).

Castro, R. R., M. Mucciarelli, G. Monachesi, F. Pacor, and R. Berardi (1999). A review of nonparametric attenuation functions computed for different regions of Italy, *Annali di Geofisica* **42,** 735–748.

Clough, R. W., and J. Penzien (1975). *Dynamics of Structures,* McGraw-Hill, New York, 634 pp.

Console, R., B. De Simoni, and A. Di Sanza (1988). Riesame della relazione magnitudo-durata, in *Atti del 7° Convegno Annuale del Gruppo Nazionale di Geofisica della Terra Solida, Roma,* 30 November–2 December 1988, 51–62.

Crosson, R. S. (1972). Small earthquakes, structure, and tectonics of the Puget Sound region, *Bull. Seism. Soc. Am.* **62,** 1133–1171.

Ekström, G., A. Morelli, E. Boschi, and A. Dziewonski (1998). Moment tensor analysis of the Central Italy earthquake sequence of September–October 1997, *Geophys. Res. Lett.* **25,** 1971–1974.

Frankel, A., A. McGarr, J. Bicknell, J. Mori, L. Seeber, and E. Cranswick (1990). Attenuation of high-frequency shear waves in the crust: measurements from New York state, South Africa, and Southern California, *J. Geophys. Res.* **95,** 17,441–17,457.

Giardini, D., M. di Donato, and E. Boschi (1997). Calibration of magnitude scales for earthquakes of the Mediterranean, *J. Seismology* **1,** 161–180.

Hanks, T. C., and H. Kanamori (1979). A moment magnitude scale, *J. Geophys. Res.* **84,** 2348–2350.

Herrmann, R. B. (1975). The use of duration as a measure of seismic moment and magnitude, *Bull. Seism. Soc. Am.* **65,** 899–913.

Hoshiba, M. (1991). Simulation of multiple-scattered coda wave excitation based on the energy conservation law, *Phys. Earth Planet. Inter.* **67,** 123–136.

Kramer, S. L. (1996). Geotechnical earthquake engineering, Prentice Hall, Upper Saddle River, New Jersey, p. 653.

Lay, T., and T. C. Wallace (1995). Modern global seismology, in Vol. 58, International Geophysics Series, Academic Press, New York, 521 pp.

Lee, W. H. K., R. E. Bennet, and K. L. Meagher (1972). A method of estimating magnitude of local earthquakes from signal duration, *U.S. Geol. Surv. Open-File Rep.*

Malagnini, L., and R. B. Herrmann (2000). Ground motion scaling in the region of the Umbria-Marche earthquake of 1997, *Bull. Seism. Soc. Am.* **90,** 1041–1051.

Malagnini, L., R. B. Herrmann, and K. Koch (2000). Regional ground motion scaling in Central Europe, *Bull. Seism. Soc. Am.* **90,** 1052–1061.

Raoof, M., R. B. Herrmann, and L. Malagnini (1999). Attenuation and excitation of three-component ground motion in Southern California, *Bull. Seism. Soc. Am.* **89,** 888–902.

Real, C. R., and T. Teng (1973). Local Richter magnitude and total signal duration in southern California, *Bull. Seism. Soc. Am.* **63,** 1809–1827.

Rovelli, A., O. Bonamassa, M. Cocco, M. Di Bona, and S. Mazza (1988). Scaling laws and spectral parameters of the ground motion in active extensional areas in Italy, *Bull. Seism. Soc. Am.* **78,** 530–560.

Sabetta, F., and A. Pugliese (1987). Attenuation of peak horizontal acceleration and velocity from Italian strong-motion records, *Bull. Seism. Soc. Am.* **77,** 1491–1511.

Sabetta, F., and A. Pugliese (1996). Estimation of response spectra and simulation of nonstationary earthquake ground motion, *Bull. Seism. Soc. Am.* **86,** 337–352.

Sole'vev, S. L. (1965). Seismicity of Sakalin, *Bull. Earthquake Res. Inst. Tokyo Univ.* **43,** 95–102.

Tsumura, K. (1967). Determination of earthquake magnitude from total duration of oscillation, *Bull. Earthquake Res. Inst. Tokyo Univ.* **15,** 7–18.

Udwadia, F. E., and M. D. Trifunac (1974). Characterization of response spectra through the statistics of oscillator response, *Bull. Seism. Soc. Am.* **64,** 205–219.

Vanmarcke, E. H., and S. P. Lai (1980). Strong-motion duration of earthquakes, *Bull. Seism. Soc. Am.* **70,** 1293–1307.

Wu, R.-S. (1985). Multiple scattering and energy transfer of seismic waves—separation of scattering effect from intrinsic attenuation. I. Theoretical modeling, *Geophys. J. R. Astr. Soc.* **82,** 57–80.

Yazd, M. R. S. (1993). Ground motion studies in the Southern Great Basin of Nevada and California, Ph.D. Thesis, Saint Louis University.

Istituto Nazionale di Geofisica
Via di Vigna Murata, 605
00143 Rome, Italy
(L. M., M. D.)

Department of Earth and Atmospheric Sciences
Saint Louis University
3507 LaClede Avenue
St. Louis, Missouri 63103
(L. M., R. B. H.)

Manuscript received 15 November 1999.